

CLLOUD-TOPPED CONVECTIVE BOUNDARY LAYERS
A REVIEW OF RECENT STUDIES

Ph. Bougeault

Direction de la Météorologie, EERM / GMD
Paris, France.

I. INTRODUCTION

The planetary boundary layer has long been known to be characterized by ubiquitous turbulence and turbulent transfers, the ultimate task of any parameterization scheme being to calculate the averaged effect of these transfers and their vertical distribution. This can be best accomplished by considering the way turbulence is generated, transported and dissipated by its own non-linear mechanics, as well as by interactions with all other relevant processes. Among these, the condensation/evaporation of water vapor plays obviously a leading role due to two main reasons : the dynamical implications of the latent heat release, and the unique radiative properties of the liquid water. The aim of this paper is to give a brief review of recent advances in these research fields.

As often as possible, the frame of the discussion will be the higher-order statistical modeling technique; this is by pure convenience. Although much information has been derived from detailed simulations of the PBL mechanics with higher-order turbulence models, it is not clear at time if such models can be of use in the framework of a GCM or a weather prediction model. However, it will be shown that this frame is well adapted and general enough to include the necessary physics, and the scale interactions, which are readily addressed by dividing the local value of each variable into a "mean" value and a turbulent fluctuation :

$$x = \bar{x} + x'$$

It is possible to derive the general rate equation for the statistical moments of x' , $\overline{x'^2}$, $\overline{x'^3}$, aso., under the assumption that the averaging operator $(\bar{\quad})$ has the comfortable properties of the ensemble averaging. In the practice, of course, this operator is not an ensemble average, but a cumbersome combination of spatial and time average. Though it is generally accepted that the final result is nevertheless of use, it must be recalled that this conclusion is subject to the so-called ergodic property. From a practical point of view, the problem is to know for which time and space scales

the theory will give the most interesting results. This question will be discussed in the last section.

The equations for the double and triple moments will not be given here. The reader is referred to classical studies by Wyngaard and Coté (1974), Zeman and Lumley (1976), or André et al. (1978), for a discussion of the closure hypothesis. A model including rate equations for the second-order moments and ad hoc parameterizations of the other terms will be called a second-order model; one including also rate equations for the third-order moments will be called a third-order model. Another assumption usually made is the horizontal quasi-homogeneity of the PBL. From experimental evidence, presented for instance by Lenschow et al. (1980), Brost et al. (1981), this is not a very strong constraint, as far as statistical homogeneity of the turbulence is only concerned. Indeed, examination of the double moments budgets shows that there is a local equilibrium of the turbulent properties and the mean profiles of temperature, humidity and wind. It means that the response time of the turbulence to an advective change in these profiles is short in comparison with the time scale of the change, at least in convective conditions. So this hypothesis of quasi-homogeneity does not prevent the theory to describe many of the meteorologically significant events at synoptic or even at meso-scale, like the horizontal convergence of mass, moisture and heat in the boundary layer.

Two regimes of the quasi-homogeneous cloudy PBL have been extensively studied in the last few years : the cumulus-topped undisturbed trade-wind layer, and the stratocumulus-topped mixed layer of the cool coastal dry climate. Other experimental results are available from the AMTEX and GATE field experiments, but a large number of theories have concentrated on the formers. Section 2 will be devoted to the treatment of the interactions between turbulence and condensation. Section 3 will emphasize some effects of the radiative transfers in the presence of clouds. Finally, Section 4 will focus on other types of motions, which could be described by the higher-order statistical equations, though not generally accepted under the topic of turbulence (internal waves, meso-scale structures). This is a more tentative section, since although satellite pictures clearly show these phenomena to be frequent, few theories have been proposed until now.

2. TURBULENT TRANSPORTS WITH PHASE CHANGES

2.1 Phenomenology

The simplest way to explain the mechanisms by which clouds interact with the turbulent transports is to consider the path of a given air parcel inside a near well-mixed environment, as outlined by Bett (1973) or Schubert et al. (1979). We consider a well-mixed subcloud layer, (i.e. where $ds/dz = 0$, s being the dry static energy $C_p T + gz$), surmounted by a cloud layer in moist adiabatic equilibrium (i.e. where $dh/dz = 0$, h being the moist static energy $C_p T + gz + Lq$). A surface originating parcel, supposed to be slightly warmer and moister than the environment, rises by buoyancy effect. If the entrainment, or turbulent mixing, of environmental air into the parcel is so weak that the parcel can preserve its individuality during the described cycle, it will experience the following effects :

.When the parcel reaches its own lifting condensation level (LCL), determined by its temperature and humidity, it starts releasing its latent heat. As the LCL of individual parcels is never very different from the mean LCL, or cloud base, the parcel then evolves in an environment characterized by a moist adiabatic lapse rate. Therefore, the heating by release of latent heat is a differential effect, converting a moisture excess into a temperature excess.

.The release of latent heat goes on until a certain height in the cloud layer is reached. Then the parcel encounters dryer air and starts to evaporate its liquid water, in the process of mixing with environment. This cools the parcel which soon becomes negatively buoyant.

.When the whole kinetic energy has been lost, the parcel begins to sink with a lower moisture content and temperature than the environment. So, it is warmed more rapidly by the pressure work than the environmental lapse rate. If it nevertheless remains negatively buoyant until the ground, it can accumulate a new amount of moisture and heat and enter a new cycle. This is a purely convective case.

.Another behaviour is possible: It can become warmer than the environment before ground. In this case, the mixing will not go on unless another energy source is present, such as shear instability. Shear originating turbulence can bring the parcel downward, where it loses sensible heat and gains moisture. This happens, for instance, in the stratocumulus regime over cold sea.

A remarkable fact is the similarity between convective processes in cumulus and stratocumulus regimes. The ultimate difference between

them does not lie in these mechanisms or in the air sea temperature difference, but in the profiles of the moist static energy h , or its linearized boundary layer form, the equivalent potential temperature θ_e , and of the total moisture content q_w . In the case of a stratocumulus, θ_e and q_w appear to be nearly well mixed. In a cumulus layer, they decrease significantly with height. Cumulus convection tends to mix θ_e and q_w , as well as stratocumulus convection, but this state will never be reached, because of entrainment of upper air with lower values of θ_e and q_w .

As a consequence, the effect of cloud non-precipitating convection is always an upward transport of moisture and moist static energy, from the surface towards the dry air above. The direction of the sensible heat transport is less obvious, since it is the difference between the former. The sensible heat is mostly released in the lower part of the cloud layer, whereas the upper part is cooled by evaporation. This is equivalent to a downward transport of heat in the cloud layer. But we feel that it is partly compensated for by an effective upward transport in the updrafts. Similarly, the associated flux of virtual temperature, or buoyancy, has different possible shapes, emphasized by Deardorff (1976). From this study, it is clear that the simple closure schemes, based on a given ratio between surface and inversion buoyancy fluxes, used in non cloudy layers, are not valid as soon as cloud convection is involved.

Another interesting problem is posed by the observed transition from stratocumulus to cumulus in the southward branch of the Hadley cell. Although this transition often appears complicated by the emergence of meso-scale convection cells, a clear concept has been outlined, called "Conditional instability of the first kind upside down" by Randall (1980), and "Cloud-top entrainment instability" by Deardorff (1980). Both authors note that, in the process of entrainment of dryer and warmer air into the stratocumulus, an entrained parcel can evaporate the surrounding liquid water, be cooled by this evaporation and continue to sink through the whole cloud layer, leading to top-driven instability. Because of the liquid water loading and the effect of water vapor on the buoyancy, the criterion for instability is not $\Delta \theta_e \leq 0$, but

$$\Delta \theta_e < \bar{T} \frac{1 + \gamma}{1 + 1.61 \gamma \epsilon} \cdot \Delta q_w < 0 \quad (n-1K) \quad \text{with } \gamma = \frac{L}{C_p} \frac{\partial q^*}{\partial T} \quad \epsilon = \frac{C_p \bar{T}}{L}$$

However, this is a local criterion derived from parcel theory or

rough entrainment hypothesis. The right question concerning cloud top instability is to know if the virtual temperature flux is positive or not at cloud top. When the virtual temperature flux associated with given mean profiles and the solid cloud cover of a stratocumulus deck becomes positive, the cloud layer reacts by explosively entraining the upper dryer air, so that the cloud is partly dissolved, and a new equilibrium is found with reduced cloud cover, insuring a negative buoyancy flux at the mean cloud top. When the instability still increases, this is soon no longer possible, and deeper, precipitating convection begins to develop.

As a result of these considerations, we need measurements and theories to elucidate the shape of the sensible and virtual heat fluxes in cloud layers.

2.2 Results from field and numerical experiments

Experimental results are available for the vertical derivatives of the sensible and moisture fluxes, or apparent heat source and moisture sink, obtained from budget studies. The fluxes themselves have rarely been measured, because of the experimental difficulty of measuring in cloudy areas. Some results are nevertheless available from Brost et al. (1981). Let us remind the usual notations, as defined for instance by Yanai et al. (1973), for the apparent heat source Q_1 , moisture sink Q_2 , and radiative heating rate Q_R :

$$Q_1 = \frac{\partial \bar{s}}{\partial t} + \nabla \cdot \underline{s\underline{v}} + \frac{\partial \bar{s}\bar{\omega}}{\partial p} = Q_R + L(C-E) - \frac{\partial}{\partial p} \overline{s'\omega'} \quad (1)$$

$$Q_2 = -L \left\{ \frac{\partial \bar{q}}{\partial t} + \nabla \cdot \underline{q\underline{v}} + \frac{\partial \bar{q}\bar{\omega}}{\partial p} \right\} = L(C-E) + L \frac{\partial}{\partial p} \overline{q'\omega'} \quad (2)$$

$$\nabla \cdot \underline{v} + \frac{\partial \bar{\omega}}{\partial p} = 0 \quad (3)$$

\underline{v} is the large-scale horizontal velocity, $\bar{\omega}$ is the vertical velocity deduced from the mass conservation equation (3), C the condensation rate, E the evaporation rate. The left-hand-side of the equations can be computed from the large-scale observations. Q_R must be evaluated from a standart radiative scheme. Integrating from the top of the atmosphere to level p , one gets the flux of moist static energy :

$$-\frac{1}{g} \overline{h'\omega'} = \frac{1}{g} \int_0^p (Q_1 - Q_2 - Q_R) dp \quad (4)$$

However, in this approach, the fluxes of sensible heat and moisture cannot be determined without a cloud model.

Nitta and Esbensen (1974) have studied with this technique the undistur-

bed period (22-26 June) of the BOMEX experiment. Their results are typical from an undisturbed trade-wind layer. Noting $p' = p - p_g$ the pressure counted from the ground, the layer from 0 to 60 mb is well mixed; a slightly stable layer extends from $p' = 60$ to 160 mb, a well-marked inversion layer from 160 to 220 mb, and a stable layer above. Under the inversion, the flow is divergent, above convergent; the subsiding mean vertical velocity has a maximum in the inversion. The Fig.1 shows the profiles of Q_1 , Q_2 , and Q_R . There is a net gain of sensible heat in the mixed layer and in the lower part of the cloud layer, and a net sink in the upper cloud layer, due to evaporation. On the other hand, there is a well marked maximum in the moisture gain under the inversion, but the gain is positive in the whole boundary layer. So, the moisture is mainly transported from the surface upward to the inversion zone to counterbalance the drying effect of the subsidence; the convective cooling of the upper layer is partly balanced by the subsident warming, but this effect is not sufficient and there is a slow destabilization of the layer, leading to an increased convective activity near the southern border of the area. Similar results have been obtained by Nitta (1976) from a situation of stratocumulus-capped mixed layer in a cold air outbreak during AMTEX 74. Complementary observations have been given by Augstein et al. (1973) from the ATBX measurements. These authors point out that the trade inversion is not a passive boundary, but the place where the mass, heat, and moisture exchanges are the largest. They further evaluated the amount of heat and moisture which is accumulated in the boundary layer and exported southward to favor deep convection in the ITCZ.

To go further in the determination of the fluxes in budget studies, one needs a cloud model. In an effort to clarify the problem, Betts (1975) has proposed to use the new variable $s_2 = C_p T + gz - Lq_l$, or liquid water static energy, (or its temperature analog $\theta_2 = \theta_e - L\bar{q}_w / C_p \bar{T}$). Betts shows that (1),(2), can be rewritten :

$$Q_1 = Q_R - \frac{\partial}{\partial p} \overline{\omega' s_2'} \quad (5)$$

$$-Q_2 = -L \frac{\partial}{\partial p} \overline{\omega' q_w'} \quad (6)$$

and gives the measured profiles of the latter quantities (Fig. 2) He further proposes a simple, efficient cloud model based on the convective mass flux parameterization. This parameterization is successfully calibrated against data from different experiments.

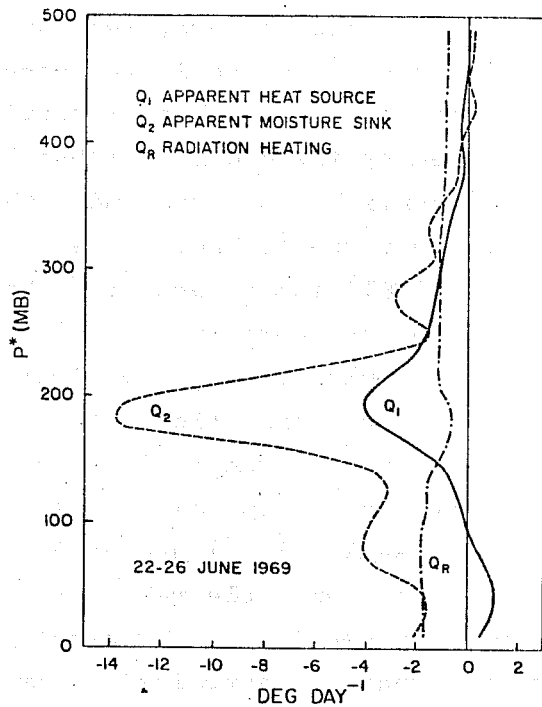


Fig.1 : Apparent heat source,moisture sink during the undisturbed period of the BOMEX experiment. (from Nitta and Esbensen, 1974)

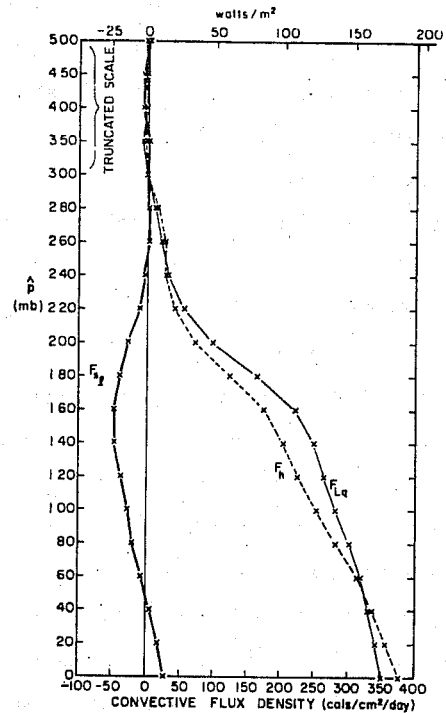


Fig. 2 : Vertical convective fluxes of moist static energy, total water and liquid water static energy. (from Betts, 1975)

The ultimate validation of this scheme should be detailed turbulence measurements in such cloudy layers. In the absence of these results, additional information can be gained from sophisticated three-dimensional simulations. Sommeria (1976) proposes a model which resolves most of the turbulent fluctuations on a grid of 50 meters mesh size. The pressure fluctuations are obtained by solving the Poisson equation for lateral cyclic boundary conditions, which is equivalent to specify the statistical homogeneity of the turbulence in horizontal planes. The equations of the motion are solved explicitly with a parameterization of the subgrid-scale eddies based on a stationary second-order turbulence closure scheme. A saturation law is introduced to allow each grid box to be saturated or not (or partially saturated in more advanced versions, according to Sommeria and Deardorff, 1977). The model is implemented for runs of a few hours, starting from rest, except for random temperature fluctuations at the surface level, and reaches a state of statistical quasi-equilibrium between the turbulent transfers and the vertical mean structure. The data generated by the model at each time step are saved and can be used to study the general

characteristics of clouds and turbulent transports, keeping in mind the possible shortcomings of such a model (truncation errors, lack of ergodicity, and non-realistic spectrum of internal waves in the stable regions). The Fig. 3 is an example of instantaneous fields of vertical velocity, moisture and liquid water produced by the model. It has been tested against aircraft turbulence measurements by Sommeria and LeMone (1978), for a case of trade-wind near Puerto-Rico (Pennel and LeMone, 1974), and by Nicholls et al. (1981) for a case from the GATE experiment. It has been used by Beniston and Sommeria (1981) to derive the general morphology of the trade-cumulus clouds, as simulated by the model, and to test successfully the parameterization scheme of Betts (1975). Redelsperger and Sommeria (1981) have generalized the model in order to allow for rain production, as a step toward the production of a deep convection model. Bougeault (1981) has used results generated by this model to derive cloud-ensemble relations for use in higher-order models (see next subsection). Eventually Deardorff (1980) has used such a model to study the entrainment rate at the top of a stratocumulus.

A similar model, but in a two-dimensional version, is used by Asai and Nakamura (1978) for the study of the air mass transformation during AMTEX. Although it is conceptually not very good to replace a 3D turbulence by a 2D turbulence, their model seems to give good qualitative results, as compared to the full 3D simulation.

2.3 Parameterization of clouds/dynamics interaction in higher-order statistical models

As a number of higher-order models of turbulence in the quasi-homogeneous boundary layer have proved to be reliable to simulate clear-sky convective processes, it was tempting to generalize these models to make them able to treat cases of cloud convection. As pointed out earlier, the main problem is to express the flux of virtual potential temperature, or buoyancy flux, the source of convection. For the stratocumulus case, Deardorff (1976) has given expressions for this flux which are valid in the cloud-free case and in the entirely cloudy case. When a non-solid cloud cover is involved, the problem is mathematically equivalent to a subgrid-scale cloudiness parameterization, as first proposed by Sommeria and Deardorff (1977), and Mellor (1977). This approach has also been investigated by Oliver et al. (1978), Banta and Cotton (1981), and Yamada and Mellor (1979). We give here a summary of the parameterization scheme proposed by Bougeault (1981), for the model of André et al. (1978). It relies upon the use of the already

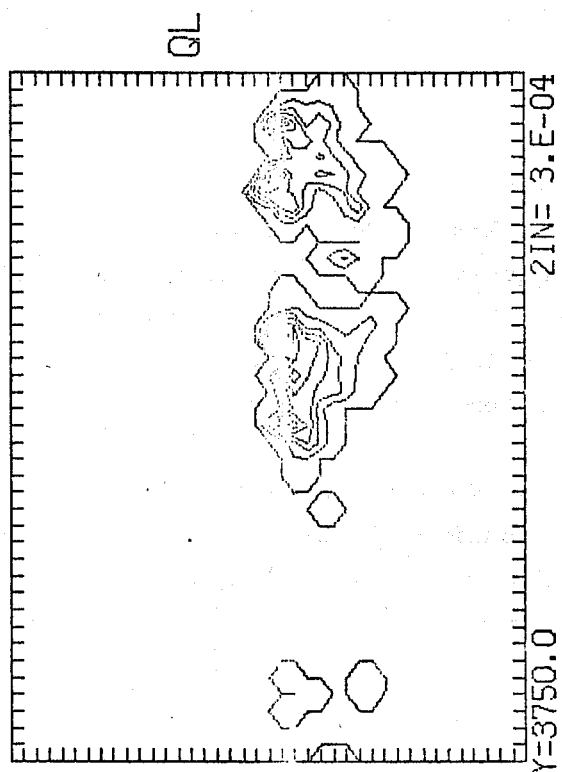
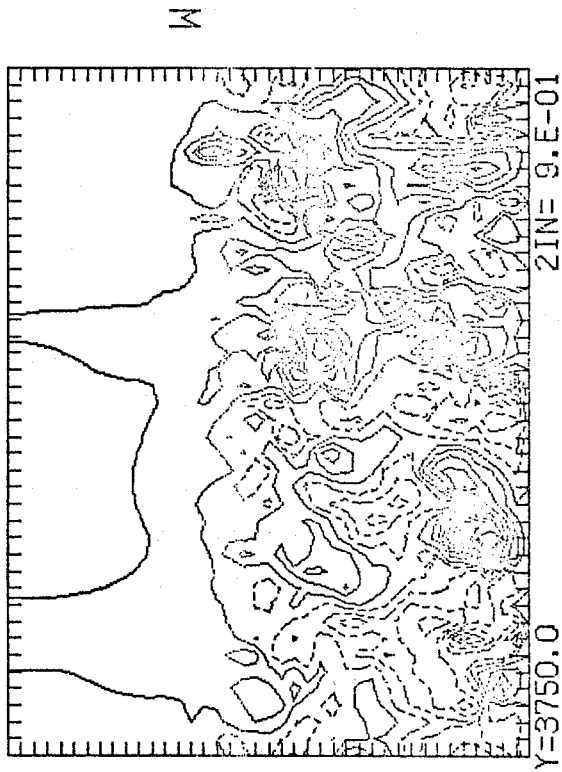
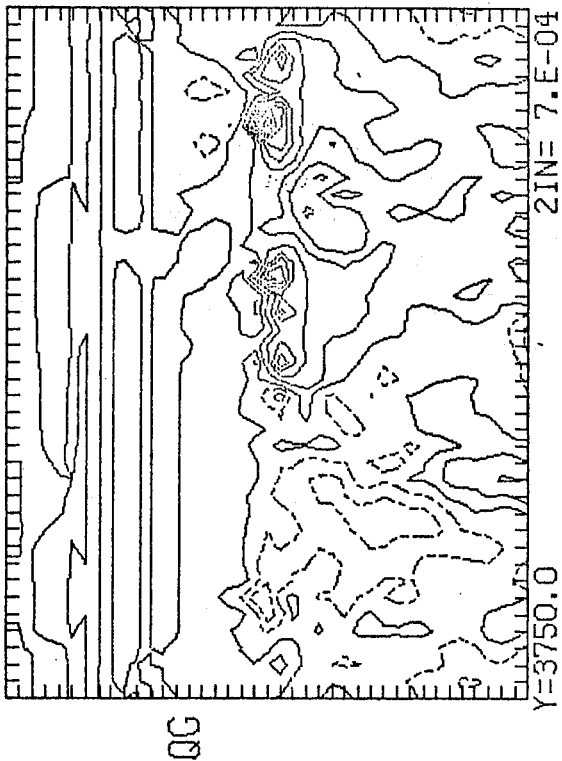


Fig. 3 : An example of the instantaneous fields of water vapor (above), vertical velocity (above right), and liquid water content (right), as produced by the 3D model. One can trace the turbulent mixed layer, capped by clouds, and the more stable layer. The length of the domain is 4 km, the height 3 km.

defined conservative variables θ_ℓ and q_w instead of θ and q in the dynamical model. (When there is no cloud, these variable reverts to θ and q , which is comfortable). The rate equations for these variables and their statistical moments are unmodified with respect to the cloud-free case except for the new definition of the virtual potential temperature

$$\theta'_v = \theta'_\ell + 0.61 \bar{T} q'_w + \{ \bar{\theta} L / c_p \bar{T} - 1.61 \bar{\theta} \} q'_\ell$$

which includes now two contributions of the liquid water (the release of latent heat minus the weight of the droplets). As the rate equations involve correlations between θ'_v and all other variables, a theory is needed to compute the correlations between q'_ℓ and these variables. Moreover, the radiative computation needs as input parameter the mean cloud cover and liquid water content $N(z)$ and $\bar{q}_\ell(z)$.

The derivation of this theory is straightforward. By linearizing the Clausius-Clapeyron equation (which is licit because the considered fluctuations are small in the boundary layer), one gets a local expression for the liquid water content :

$$q_\ell = \text{Max} (0, a(q_w - q^*(\bar{\theta}_\ell)) + 2s) \quad (7)$$

where s is a linear combination of θ'_ℓ and q'_w which controls the condensation (a confusion with the dry static energy is to avoid), first defined by Mellor (1977) :

$$s = \frac{a}{2} (q'_w - \alpha_1 \theta'_\ell)$$

where $a = (1 + \gamma)^{-1}$, $\alpha_1 = \gamma c_p / L$
with the usual notation $\gamma = L \partial q^* / c_p \partial T$

We call $t = s / \sigma_s$ the normalized centered variable describing the fluctuations of this "condensation potential" in the horizontal layer. σ_s is known from the main dynamical equations. From (7) we can easily obtain expressions for the mean cloud cover, liquid water content, and correlations between q'_ℓ and s :

$$\begin{aligned} N &= \int H(q_\ell(t)) G(t) dt \\ \bar{q}_\ell &= \int q_\ell(t) G(t) dt \\ \overline{s q_\ell} &= \int s q'_\ell(t) G(t) dt \\ \overline{s^2 q_\ell} &= \int s^2 q'_\ell(t) G(t) dt \end{aligned} \quad (8)$$

To close the theory, we need to specify the probability density function (pdf) $G(t) dt$ inside an horizontal plane. This is an appealing question, since it appears as the only degree of freedom in the theory. The first studies by Sommeria and Deardorff (1977), Mellor (1977), and Bougeault et al. (1979), assumed a gaussian law, as no other information was available. In an effort to fit the results of the 3D simulation by Sommeria, Bougeault (1981) has proposed to use a more realistic and more simple skew exponential pdf :

$$G(t) dt = H(t+1) e^{-(t+1)} dt \quad (9)$$

where $H(x)$ is the Heaviside step function. So $G(t)=0$ for $t < -1$ but this is not of any inconvenience here. This pdf has a skewness factor $t^{1/3}$ of 2. A physical explanation of the best results provided by a positive skewness is easy : in the onset of cumulus convection, the updrafts in the cloud interiors are far more violent than the downdrafts in the environment. So, though the use of conservative variables prevents to see any discontinuity due to the presence or absence of clouds, the distribution of the scalar quantities θ'_j and q'_w is skewed, due to the the skewness of the vertical velocities distribution in a stratified environment. Positively skewed distributions of vertical velocities in clouds have been confirmed by field experiments, even in stratocumulus layers (Coulman, 1978)

It is not likely, however, that the simple form (9) be universal. So, Bougeault (1981) proposes a generalized form of the theory, to include a variable skewness factor. Let us remind that this scheme is designed to be used in a third-order model, in which the skewness factor needed by the theory can be computed by the dynamical model. The generalized form of (9) is based on the Gamma function :

$$G_p(t) dt = \frac{\beta^p}{\Gamma(p)} t^{p-1} e^{-\beta t} dt \quad (10)$$

with $p = \beta^2 = 4/A_s^2$, A_s being the skewness factor. For $A_s = 2$, the scheme reverts to the simple form (9), and when A_s tends towards 0, the limit is the gaussian scheme of Sommeria and Deardorff (1977). The Fig.4 compares the parameterized value of the mean liquid water content, obtained from (8) with this form of $G(t)$, and the value computed from the individual grid points in the 3D model of Sommeria, for four different experimental cases. Each point represents the result for one horizontal plane (1600 grid points), averaged over a 20 minutes time sequence. Equivalent comparisons have been made for $\overline{sq'_e}$ and $\overline{s^2 q'_e}$.

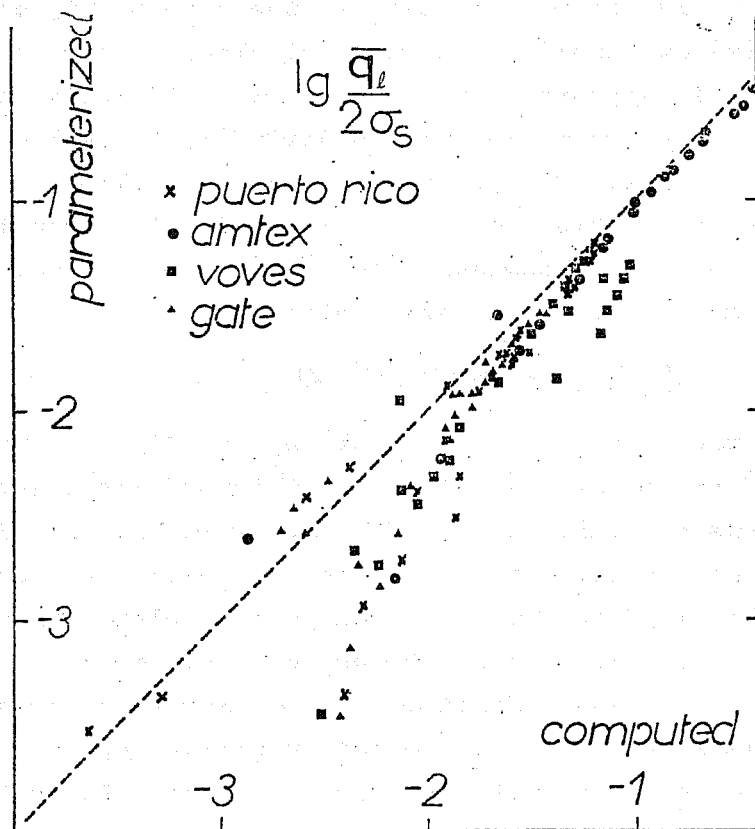


Fig.4. Test of the parameterization of the mean liquid water content. Abscissa: values computed from the 3D model Ordinate: value predicted from the scheme. From Bougeault (1981).

Turning now to the initial problem of expressing correlations between q'_e and any other variable, it is suggested to use the simple form :

$$\overline{m'q'_e} = \overline{m's} \cdot \overline{sq'_e} / \sigma_s^2 \quad (11)$$

It can be demonstrated when the joint pdf for (s,m) is gaussian. It is tempting to extrapolate the form for the non-gaussian case, since (11) produces the right limit when the cloud cover tends towards 0 or 1. In the limit of the solid cloud, indeed, $q'_e \sim 2s$, from (7), and (11) becomes $\overline{m'q'_e} = 2 \overline{m's}$. On the other hand, in the limit of small cloud covers, as observed in the initial 3D Puerto-Rico simulation, all variables have nearly bimodal distributions; with separation between in-cloud and environmental values. So, all correlations are very strong, with $\overline{m's} \sim \sigma_m \sigma_s$, and (11) reads approximately : $\overline{m'q'_e} = \frac{\sigma_m}{\sigma_s} \overline{sq'_e}$

which feels correct.

As a conclusion, Fig. 5 shows the results of the parameterization of $\overline{m'q'_e} / 2 \sigma_s^2$, for different values of the input parameters $Q_1 = \frac{a(q_w - q^*(\bar{c}_e))}{2\sigma_s}$

and A_s , the skewness factor. Clearly, the influence of A_s for a fixed Q_1 is very strong for low Q_1 (small cloud covers), and becomes negligible for large Q_1 (near stratocumulus regime): there, all probability density functions give the same results. It is therefore suggested that, for models which have no third-order moments to compute the skewness factor, the initial proposition (9) can provide a valuable improve of the description of the cumulus regime, without any bad influence over the other regimes. This pdf leads to the following useful formulae:

$$N = e^{Q_1 - 1} \quad 1$$

$$\frac{\overline{q_e}}{2\sigma_s} = e^{Q_1 - 1} \quad \text{if } Q_1 \leq 1 \quad Q_1 \quad \text{if } Q_1 \geq 1 \quad (12)$$

$$\frac{\overline{sq_e}}{2\sigma_s^2} = (2 - Q_1) e^{Q_1 - 1} \quad 1$$

for $Q_1 = a(q_w - q^*(\theta_e)) / 2\sigma_s$

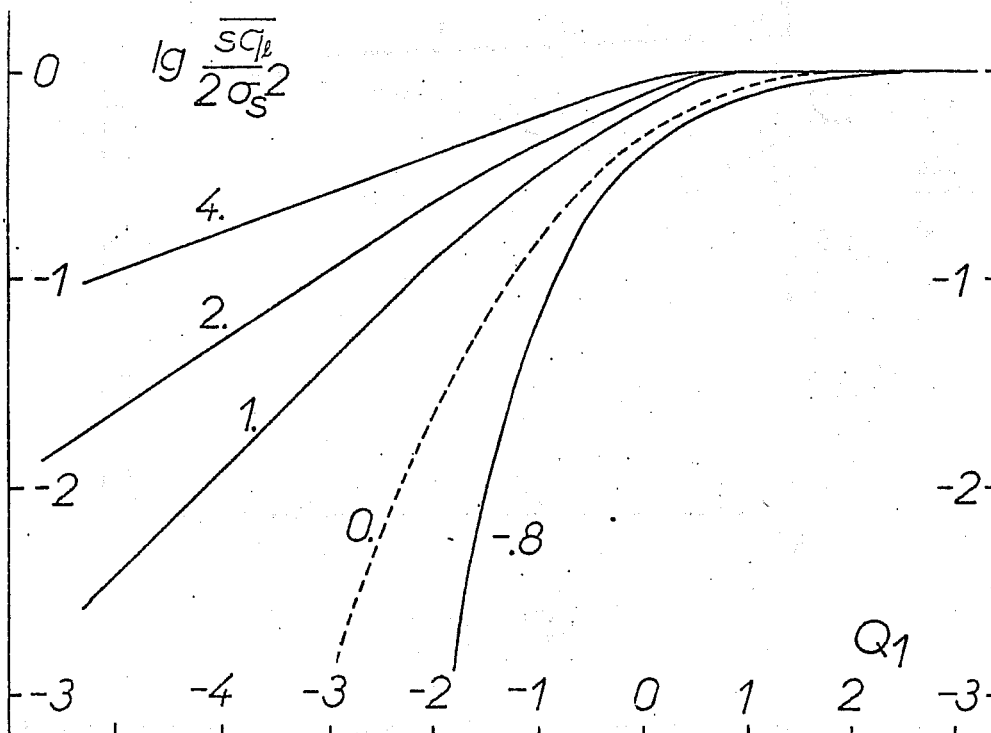


Fig.5 : Parameterized value of the second-order correlation $\overline{sq_e} / 2\sigma_s^2$. Different curves stand for different values of the skewness factor. For $A_s=0$, gaussian scheme (dashed curve).

This simple scheme has been used by Bougeault (1981) to reproduce with a third-order statistical model the cumulus convection, as calculated by the 3D model, with fairly good agreement. All profiles of the double and triple moments were obtained with reasonable accuracy. Fig. 6 and 7 are from this study and show the profiles of the temperature variance $\overline{\theta'_\ell{}^2}$ and its vertical transport $\overline{w'\theta'_\ell{}^2}$. The variance is shown to have a strong maximum near 1400 m, i.e. the trade inversion; significant values are maintained in the whole cloud layer (from 500 to 1400 m), and small values under this level, fitting the idea of "well-mixed" layer. The transport $\overline{w'\theta'_\ell{}^2}$ shows that the variance is carried upward by the clouds. It is to be noted that any assumption of gradient diffusion would fail in this case : convective processes seem to be invariably associated with complex turbulent transports !

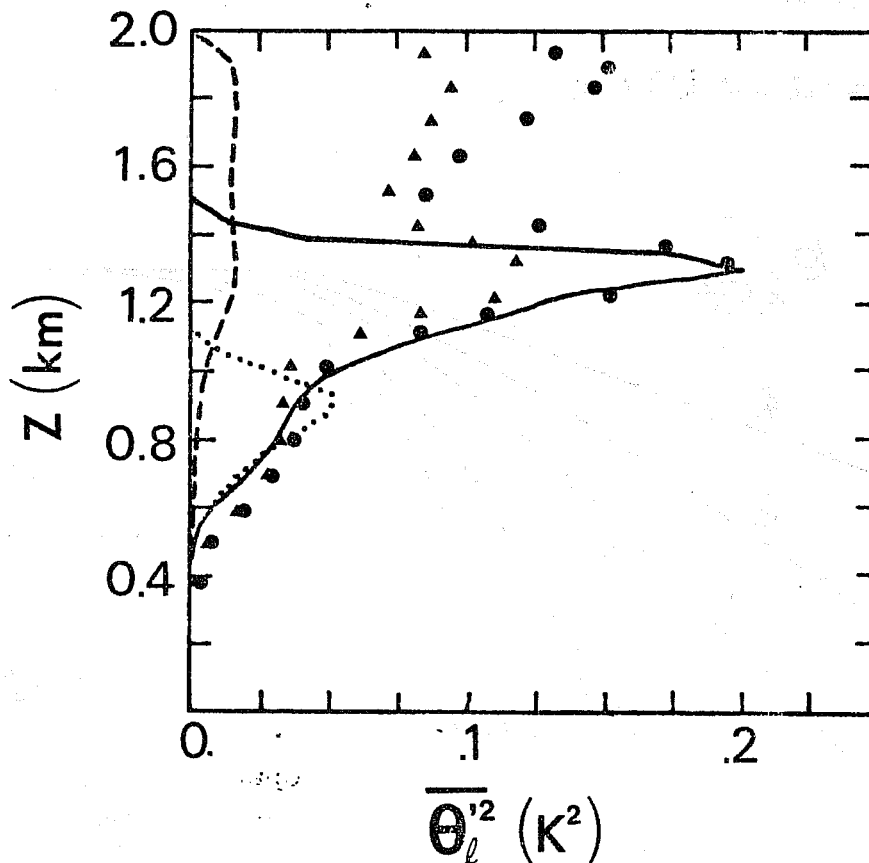


Fig. 6: Vertical profile of the temperature variance in the simulation of Puerto-Rico data. Full line: LD model; dotted line: LD model with gaussian parameterization; symbols: 3D results; triangle and circles stand for two slightly different time sequences of average and give an idea of the variability of the 3D results.

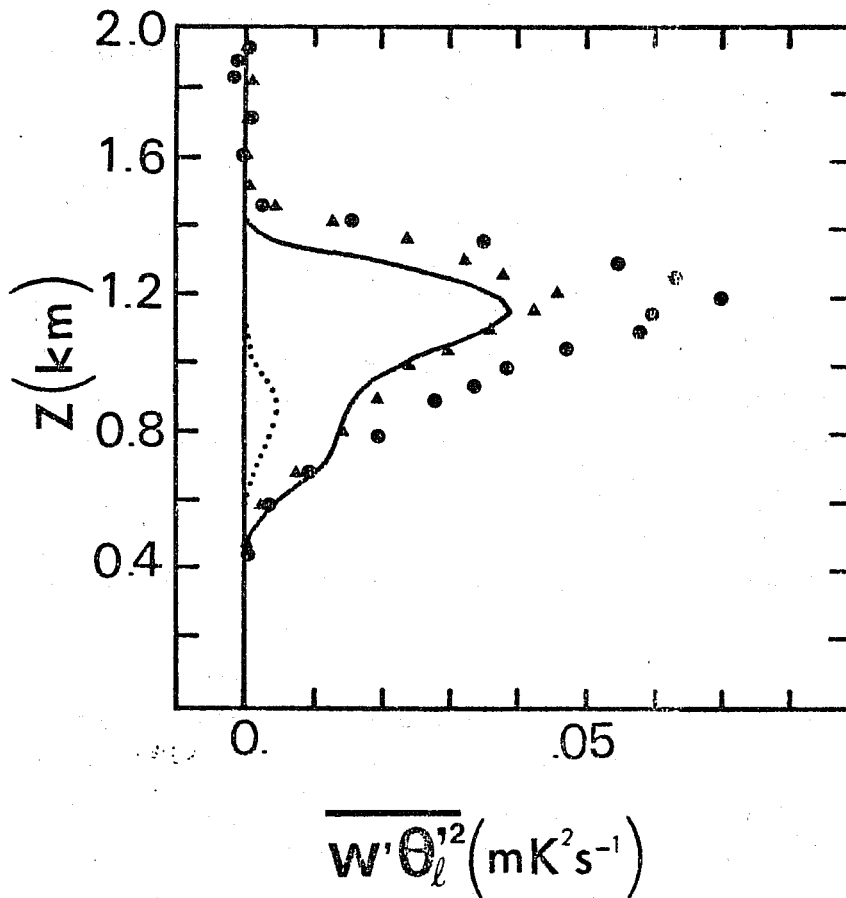


Fig. 7: As in Fig.6, for the vertical transport of temperature variance. (from Bougeault, 1981)

3. RADIATIVE TRANSFERS IN CLOUDY LAYERS

Clouds have long been considered in the models to have the properties of a blackbody. Recent studies, however, agree to consider that the longwave radiative transfers can be adequately computed by assuming the liquid water to have a greybody emissivity :

with $k \sim 120-150 \text{ kg}^{-1} \text{ m}^2$ and $W = \int p q dz$ the integrated liquid water path (Stephens, 1978; Morcrette, 1977; Fouquart et al., 1980)

On the other hand, the shortwave radiative transfer computation needs a parameterization of the diffusion, which is very sensitive to the droplet size spectrum. It is not our intention, however, to give a discussion of the different radiative schemes. All schemes agree to predict that the effect of infra-red radiation is to cool strongly the top of the clouds (typically 10 K per hour, localized in the top 50 meters), and possibly warm the bottom of the thicker clouds. Solar radiation warms the whole cloud, at a smaller rate, typically 2 K per

hour, but the extinction length of this heating in the cloud is much larger than for the infra-red cooling, so that the net radiative effect at some height below the cloud top may be a net heating.

This acts on the mean profiles and can generate or inhibit turbulence through stability, or cloud development through a change in the mean saturation value of the humidity. These interactions are taken into account in most of the proposed models, either explicitly, in the 3D or higher-order models, or implicitly, in the parametric models, where it is often assumed that the sum of the turbulent and radiative fluxes of heat is linear. Other possible interactions between turbulence and radiation will be addressed in a further section.

3.1 Effects of radiation through changes in the mean profiles

It has been noted that the global effect of cloud convective transfers was an evaporative cooling of the upper cloud layer, where cloudy air continuously mixes with entrained dry air. Radiation enforces the phenomenon in this region where the infra-red cooling dominates the solar heating. In the lower cloud layer radiation and convection again play the same role, since residual solar radiation and infra-red ground effect result in a weak warming. So, radiation is generally supposed to enhance the convective mechanisms, without much modification.

A few words should be said about the recent polemic concerning the location of the radiative cooling in a stratocumulus topped mixed layer. Whereas Lilly's (1968) initial model assumed the cooling to be concentrated in a layer of infinitesimal thickness just above cloud top, Deardorff (1976) and Schubert et al. (1979) allow a certain amount of cooling to occur within the cloud. Moreover, Kahn and Businger (1979) argue that the cooling is an integral part of the cloud layer, and that the concept of radiative discontinuity is not satisfactory, because the implicit effect over the turbulent flux of heat is badly predicted. Deardorff (1981) claims that a certain amount must be preserved as a discontinuity in order to allow for cloud-top irregularities in the frame of the Reynolds averaging.

In an effort to clarify the problem, Lilly and Schubert (1979), Randall (1980), and Deardorff (1981) have investigated the sensitivity of the stationary solutions to these hypothesis. The general result is not optimistic : Randall shows that in the cases of cold water surface, strong subsidence, or weak value of the entrainment parameter, the cloud depth depends strongly on the assumed value of the radiative

divergence depth. Moreover, for large value of this last parameter, the sensitivity of the model results to the entrainment hypothesis is also increased. Deardorff (1980) has computed that if h is the depth of the mixed layer, and λ the depth of the radiative divergence zone, the vertically integrated virtual temperature flux (i.e. the total buoyancy production) depends upon h/λ and has a maximum for $h/\lambda \sim 10$. This can be explained in such terms: if λ is too small, the radiative cooling is restricted to the cloud top, where its effect is locally compensated by the entrainment. If λ is too large, the radiative cooling extends to the whole cloud layer, and fails to generate the instability which increases the buoyancy flux.

The last step was to compute directly the infra-red and solar radiative effect for realistic profiles of all relevant parameters. This has been accomplished by Fravallo et al. (1981). These authors have implemented a parametric model of stratocumulus-capped mixed layer, with detailed radiative computations. Their results confirm the important role played by the optical thickness of the cloud, and by the drop size distribution. Moreover, the sensitivity of the model to the short wave heating suggests a significant diurnal cycle.

How relevant are all these results from the point of view of higher-order statistical modeling? It must be noted first that a way of taking the radiative transfers into account coherent with the computational complexity of the higher-order modeling is to compute directly the cooling rate from the emissivity approximation. However, the former studies show that a very high resolution near cloud top is probably needed to gain information from these complicated computations. Such a resolution is not compatible with the requirements of a GCM. The question is therefore open. A possible advance could be brought by the NEPHOS project: A number of cases of stratocumulus, investigated from satellite pictures and large-scale model analysis will be studied with the aid of high resolution boundary layer models, in order to derive the stability and radiative properties of these clouds. The results should be used to design a comprehensive parameterization of the stratocumulus topped boundary layer.

Another effect of radiation is a possible diurnal cycle investigated by Albrecht et al. (1979), and Augstein et al. (1980), for the trade-wind cumulus case. By increasing the humidity saturation value, the solar heating suppresses cloud development and results in lower cloud top levels. Consequently, the clouds have a maximum in the early morning hours. At this time, the moisture supplied by surface evaporation

is transported directly at cloud top to feed this development. The moisture in the mixed layer can even decrease in this process, whereas the total moisture amount of the layer increases. During the afternoon, the clouds are pushed downward by the subsidence, and moisture is accumulated in the mixed layer, resulting in a reduced surface evaporation. Concerning this behaviour, the results of the model study by Augstein correspond to the observations during the ATEX experiment, although a somewhat larger response time is observed in the model. The observed cycle in the mean subsidence is shown to have few effects on the cloud height. On the contrary, the model study by Albrecht shows the solar radiation to be insufficient to explain the observed variation in the cloud top height. The right behaviour is recovered with a somewhat larger amplitude in the assumed mean subsidence cycle. A possible explanation of this discrepancy between both models is that the cloud cover is supposed to be constant in the study by Albrecht. Interestingly, the associated diurnal amplitudes of the temperature variations predicted by both models agree to be 0.5 K

Similar results have been noted by Oliver et al. (1978) for the Californian stratocumulus, indicating a maximum at the end of the night and a minimum at the end of the day, in an opposite way with the clear-sky convective boundary layer.

3.2 Interactions with radiation not reducible to changes in the mean profiles

Whereas the horizontally averaged effect of the radiative cooling at the top of a cloud layer has been extensively studied, few contributions have addressed the problem of the influence of local fluctuations of the cooling, linked to variations in the concentration of the liquid water, seen as a greybody. This question is particularly appealing in the case of a cumulus layer, since the radiative cooling in this case occurs at the top of the individual clouds, and can interact with dynamics more strongly than if it were horizontally distributed. An investigation of this effect is presented by Veyre et al. (1980). The authors have modified the 3D model of Sommeria (1976) in order to allow for a computation of the radiative transfers inside each vertical column. This modification seems to increase convective activity, and results in somewhat larger cloud covers and fluxes, as shown by Fig.8. In the reference run, however, denoted as "transparent clouds" in the figure, the radiative cooling was simply assumed to be the clear-air one. So, it is not clear if a radiative computation with a mean cooling rate, taking into account the mean cloud emission, would not have

produced a similar increase in the convection. Complementary results will be given in a forthcoming paper. Moreover, if such modifications were to be maintained for long-term integrations of the model, one would have to take it into account in the higher-order modeling technique.

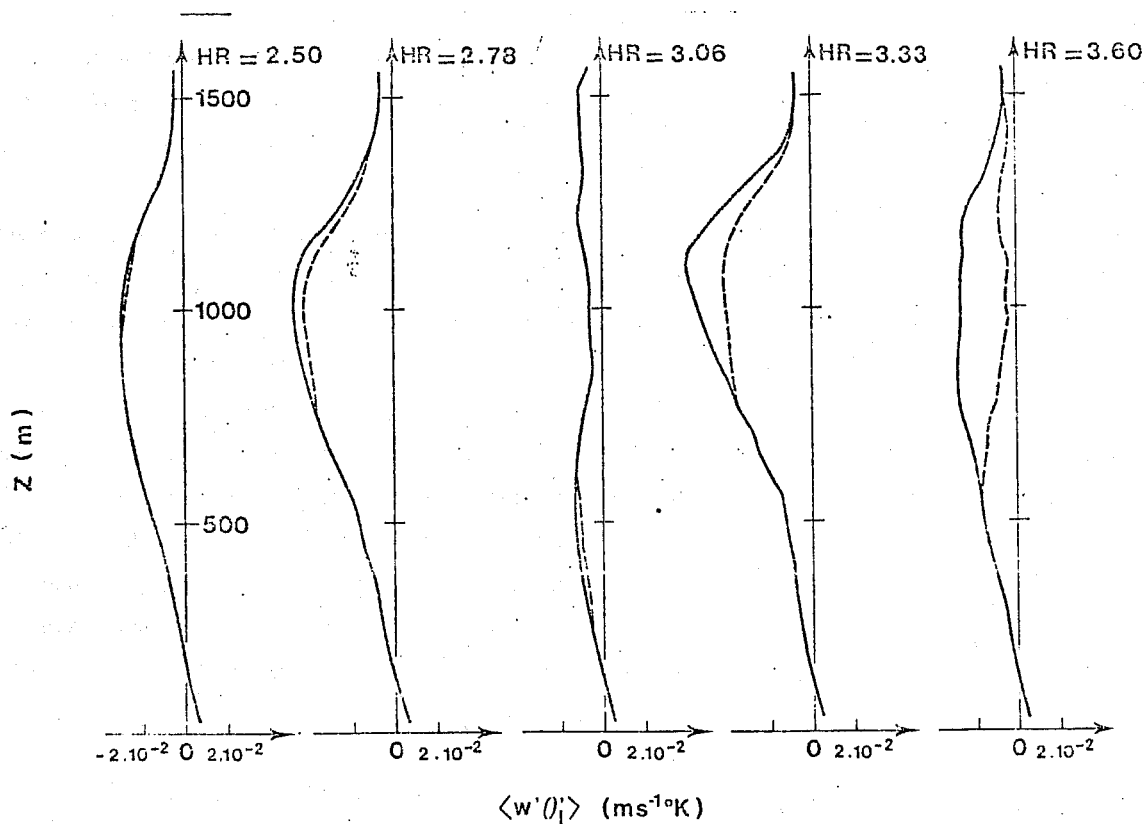


Fig. 8 : Vertical flux of liquid water temperature $\overline{w'\theta'_l}$ as produced by the 3D model; full lines: interactive clouds; dashed lines: transparent clouds.

If R is the local value of the radiative heating or cooling rate, it can be divided into a mean value and a fluctuation : $R = \overline{R} + R'$
 \overline{R} is computed from the classical radiative scheme, assuming horizontal homogeneity. R' is taken into account by its correlations with the other variables, for instance in the rate equation for the temperature flux :

$$\frac{\partial}{\partial t} \overline{w'\theta'_l} = \{ \dots \} + \overline{w'R'}$$

So, one needs a scheme to compute the correlations between R' and the other variables. The section 2.3 has shown that it is easy to evaluate correlations between q'_l and s , which measures the condensation potential. As fluctuations R' are most likely due to the fluctuations in the liquid water content q'_l or even in the water vapor content, correlations between R' and s will probably be of interest. The difficulty, in this

computation, is R' is determined, not only by local values, as was q'_z in section 2.3, but by the vertically integrated content of all absorbants. One has to make an additional assumption, concerning the way the fluctuations in q'_z are correlated along the vertical. Assuming some simple form for this information, it should be possible to derive an expression for $\overline{SR'}$, which would represent our intuitive feeling, that the regions where the liquid water has its maximum concentration are also the regions which are most intensively cooled by radiation, if only they are not surmounted by large amounts of clouds.

Fluctuations in the cooling rate are not the only effect of interaction between turbulence and radiation. André et al. (1978) have early noted that the horizontal radiative exchanges must result in a damping of the temperature variance $\overline{\theta'^2}$. Simonin (1981) and Schertzer and Simonin (1981) have addressed the dissipation of temperature variance in an isotropic homogeneous turbulence with radiative transfers. Their work shows that the radiative exchanges result in an equivalent diffusivity K_{rad} for the large scale temperature fluctuations. It is then possible to define a radiative Prandtl number $P_{rad} = \nu / K_{rad}$, and, under certain conditions on P_{rad} , the temperature fluctuations spectrum is strongly affected; in such cases, the dissipation hypothesis in the higher-order models should be revised.

One of the aim of this section was to show that interaction between cloud turbulence and radiation is a widely open research field. It is to hope that all these interactions can be taken into account in the framework of higher-order modeling, with only minor revisions. However, a strong limitation will probably be set by the high needed resolution.

4. TURBULENCE AND OTHER MOTIONS

As discussed in the introduction, this section addresses some recently investigated problems related to the interaction between turbulence and other motions. Among these, small scale internal waves and meso-scale structures are the most important. A complete review should include a discussion of the study by LeMone (1976) of roll-modulated turbulence. From a practical point of view, we shall include these rolls into the turbulence, as described by the higher-order models.

We are lead to these considerations by the structure of the higher-order turbulence equations, which are general enough to include any type of motion, at least before any closure assumption is made. The modeler

has to make his own choice, with respect to what type of motions or variability he wants to include in the "turbulent" description, and what type he does not want.

4.1 Internal waves in the statistical models ?

Many experimental investigations of internal waves in the boundary layer have been reported (see e.g. Einaudi et al.(1979) for a review) either trapped in an inversion layer, or with significant vertical phase velocity. These waves are shown to be generated by various sources, local, as wind shear at the inversion, or buoyancy originating turbulence, or non-local, as distant storms or fronts. They can be associated with significant vertical transports of momentum and energy and should be included into the parameterization of the PBL, especially the nocturnal PBL. Moreover, the frequently observed breaking of a wave is a typical example of wave/turbulence interaction. The question is therefore : how should the higher-order schemes be modified in the statically stable regions to be able to represent these waves ?

Although much is known concerning the properties of internal waves, few contributions have tried to answer it. Some information can be gained from results in the oceanic boundary layer, or thermocline. Kantha (1977) has developed a parameterization of the vertical energy flux due to the internal waves in the ocean. Bougeault (1980) proposes a more simple, but similar approach, based on a simple linear free wave in a region of constant stability, or Brunt-Väisälä frequency N . It is possible to draw a relation between the energy flux and the vertical velocity variance :

$$\overline{w'p} = N \operatorname{tg} \theta \overline{w'^2} / k$$

where θ is the direction of propagation of the wave, counted from the horizontal, and k the horizontal wave number. The idea is to use this simple form to parameterize the usually neglected correlation $\overline{w'p}$ in a higher-order model. More information, however, could be gained with a more realistic model of wave. One of the results of this rough approach is that the pressure associated energy flux is likely to play a role in energy propagation in a stably stratified layer. Other informations can be brought by the 3D simulations by Deardorff (1980, 1974). Let us remember that the non-hydrostatic pressure fluctuation is effectively computed in this model from its Poisson equation. Mean profiles of $\overline{w'p}$ shown by Deardorff support the idea of an energy propagation from the boundary layer towards the free atmosphere. Mason and Sykes' (1981) two-dimensional small scale model similarly shows that internal waves can interact with rolls at the top of the boundary layer, transferring upward, or downward a

10-20 % of the surface turbulent fluxes of heat and momentum. Some recent advances have been directed towards the experimental study of this interaction (Einaudi and Finnigan, 1981; Finnigan and Einaudi, 1981; Merrill and Grant, 1979), linear numerical models to determine the structure of the waves associated to given profiles of mean shear and stability (Merrill, 1977), and 3D direct simulations of the waves.

4.2 Meso-scale variability of the boundary layer

Whereas in the preceding section we were confronted to the question of including or not including the internal waves in the turbulent description, the problem in this section is : what is the maximum horizontal scale of the fluctuations accounted for by the higher-order equations ? In other terms, for what horizontal scales are the averaging operators representative ? The answer is not obvious. On continental surfaces, a major constraint is set by the ground characteristics. As far as the boundary layer over ocean is concerned, only experimental evidence can give informations.

The most clear evidence of meso-scale variability is obtained, once again, for cloudy layers. Pennel and LeMone (1974), from their already cited airborne investigation of the trade-wind near Puerto-Rico, point out the existence of patches of cloud-free areas, suppressed convection areas, and active convection areas, each having an horizontal extension of approximately 40 km. The model simulation by Sommeria and LeMone (1978), as well as its 1D counterpart by Bougeault (1981), are clearly representative of only one of these domains. On the other hand, a rough calculation of the available moisture by LeMone and Pennel (1976) supports the idea of a continual evolution of the cloud patches, which "pump" the moisture of the mixed layer, before progressing towards a place where moisture is available. Accordingly, the moisture flux is weak in the suppressed areas, and strong in the active areas. The possibility of including this variability in a similar technique as described in section 2 is an open question. Other observations of variability in a scale of 10 km in the fair weather boundary layer during GATE experiment have been reported by Nicholls and LeMone (1980). However, no fluxes were associated with these scales. Among other explanations, these inhomogeneities might have been produced by more active, deeper convection in the hours before the observations.

A complete set of observations on meso-scale cellular convection during AMTEX 75 is given by Rothermel and Agee (1980). These authors present airborne measurements of humidity, temperature and velocity on a flight

track crossing closed cells of approximately 40 km diameter, at a 1 km altitude. Their conclusions prove the existence of a well-defined cell-scale circulation, with a mean vertical velocity of 1 ms^{-1} upward at the center of the cell, and differences between inner and outer values of the parameters being roughly $\Delta q = 1 \text{ gKg}^{-1}$, $\Delta T = 0.25 \text{ K}$, and $\Delta u = 1.5 \text{ ms}^{-1}$. The fig.9 emphasizes the proposed model for the cell structure. Clearly a 1D higher-order statistical model can be representative of the mean conditions in the ascending, cloudy branch of the cell, or in the subsiding, cloud-free walls. But how about the possibility of representing the averaged phenomenon with such a model? In this extreme example, a combination of two simpler models, with respectively stratiform clouds and no clouds may be more usefull than a model with partial cloudiness. If this has nevertheless to be accounted for in the framework of 1D hihger-order modeling, the closure assumptions of the model could have to be revised in a significant way. For instance, the amount of energy associated with the cell-scale motions suffers from less dissipation than if the same energy was under a purely turbulent form. The distribution laws proposed in section 2 may have also to be changed.

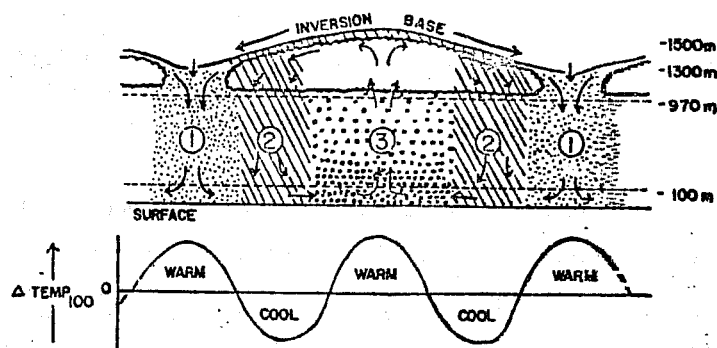


Fig. 9 : The structure of a closed convective cell during AMTEX 75. (from Rothermel and Agee, 1980)

REFERENCES

- André, J.C., G. De Moor, P. Lacarrère, G. Therry, and R. Du Vachat, 1978: Modeling the 24 h evolution of the mean and turbulent structures of the planetary boundary layer. J. Atmos. Sci., 35, 1861-1883.
- Asai, T., and K. Nakamura, 1978: A numerical experiment of Air mass transformation processes over warmer sea. Part I: Development of a convectively mixed layer. J. Meteor. Soc. Japan, 56, 424-434.
- Augstein, E., H. Riell, F. Ostapoff, and V. Wagner, 1973: Mass and energy transports in an undisturbed atlantic trade-wind flow. Mon. Wea. Rev., 101, 101-111.
- Augstein, E., and M. Wendel, 1980: Modelling of the time-dependent atmospheric trade-wind boundary layer with non-precipitating cumulus clouds. Beitr. Phys. Atmosph., 53, 509-538.
- Banta, R., and W.R. Cotton, 1981: On computing average cloud-water quantities in a partially cloudy region. J. Rech. Atmos., special issue, May 1981.
- Beniston, M., and G. Sommeria, 1981: Use of a detailed planetary boundary layer model for parameterization purposes. J. Atmos. Sci., 38, 780-797.
- Betts, A. K., 1973: Non precipitating cumulus convection and its parameterization. Quart. J. Roy. Meteor. Soc., 99, 178-196.
- Betts, A.K., 1975: Parametric interpretation of trade-wind cumulus budget studies. J. Atmos. Sci., 32, 1934-1945.
- Bougeault, Ph., G. Sommeria, and J.C. André, 1979: Méthode de modélisation unidimensionnelle de la couche limite planétaire nuageuse ; Comparaison avec un modèle tridimensionnel. J. Rech. Atmos., 13, 249-259.
- Bougeault, Ph., 1980: Modélisation unidimensionnelle de la couche limite tropicale nuageuse. Thèse de 3è cycle, Université Paris VI.
- Bougeault, Ph., 1981a: Modeling the trade-wind cumulus boundary layer. Part I: Testing the ensemble cloud relations against numerical data. to appear in J. Atmos. Sci.
- Bougeault, Ph., 1981b: Modeling the trade-wind cumulus boundary layer. Part II: A high-order one dimensional model. to appear in J. Atmos. Sci.
- Bougeault, Ph., 1981: Cloud-ensemble relations for use in higher-order models of the planetary boundary layer. (submitted to J. Atmos. Sci.)
- Brost, R. A., D.H. Lenschow, and J.C. Wyngaard, 1981: Marine stratocumulus layers. Part I: Mean conditions. (submitted to J. Atmos. Sci.)
- Brost, R.A., J.C. Wyngaard, and D.H. Lenschow, 1981: Marine stratocumulus layers. Part II: Turbulence budgets. (submitted to J. Atmos. Sci.)
- Coulman, C.E., 1978: Convection in stratiform clouds. J. Rech. Atmos., 12, 21-33.

- Deardorff, J.W., 1974: Three-dimensional numerical study of turbulence in an entraining mixed layer. Bound.-Layer Meteor., 7, 199-226.
- Deardorff, J.W., 1976: On the entrainment rate of a stratocumulus-topped mixed layer. Quart. J. R. Met. Soc., 102, 563-582.
- Deardorff, J.W., 1980: Cloud Top Entrainment instability. J. Atmos. Sci., 37, 131-147.
- Deardorff, J.W., 1980: Stratocumulus-capped mixed layers derived from a three-dimensional model. Bound.-Layer Meteor., 18, 495-527.
- Deardorff, J.W., 1981: On the distribution of mean radiative cooling at the top of a stratocumulus-capped mixed layer. Quart. J. Roy. Met. Soc., 107, 191-202.
- Einaudi, F., D.P. Lalas, and G.E. Perona, 1979: The role of gravity waves in tropospheric processes. Pageoph., 117, 627-663.
- Einaudi, F., and J.J. Finnigan, 1981: The interaction between an internal gravity wave and the planetary boundary layer. Part I: The linear analysis. Quart. J. Roy. Met. Soc., 107, 793-806.
- Finnigan, J.J., and F. Einaudi, 1981: The interaction between an internal gravity wave and the planetary boundary layer. Part II: Effect of the wave on the turbulence structure. Quart. J. Roy. Met. Soc., 107, 807-832.
- Fouquart, Y., and E. Bonnel, 1980: Computations of solar heating of the earth's atmosphere: a new parameterization. to appear in Contrib. Atmos. Phys.
- Fravelo, C., Y. Fouquart, and R. Rosset, 1981: The sensitivity of a model of low stratiform clouds to radiation. J. Atmos. Sci., 38, 1049-1062.
- Kahn, P.H., and J.A. Businger, 1979: The effect of radiative flux divergence on entrainment of a saturated convective boundary layer. Quart. J. Roy. Meteor. Soc., 105, 303-306.
- Kantha, L.H., 1977: Note on the role of internal waves in thermocline erosion. in "Modelling and prediction of the upper layer of the ocean" E.B. Kraus, Pergamon Press, pp. 173-177.
- LeMone, M.A., 1976: Modulation of turbulence energy by longitudinal rolls in an unstable planetary boundary layer. J. Atmos. Sci., 33, 1308-1320.
- LeMone, M.A., and W.T. Pennel, 1976: The relationship of trade-wind cumulus distribution to subcloud layer fluxes and structure. Mon. Wea. Rev., 104, 524-539.
- Lenschow, D.H., J.C. Wyngaard, and W.T. Pennel, 1980: Mean-field and Second-moment budgets in a baroclinic, convective boundary layer. J. Atmos. Sci., 37, 1313-1325.
- Lilly, D.K., 1968: Models of cloud-topped mixed layers under a strong inversion. Quart. J. Roy. Meteor. Soc., 94, 292-309.
- Mason, P.J., and R.I. Sykes, 1981: A two-dimensional numerical study of horizontal roll vortices in an inversion capped planetary boundary layer. to appear in Quart. J. Roy. Met. Soc.
- Mellor, G.L., 1971: The gaussian cloud model relations. J. Atmos. Sci., 34, 356-358. See also Corrigenda J. Atmos. Sci., 34, 1483-1484.

- Merrill, J.F., 1977: Observational and theoretical study of shear instability in the airflow near the ground. J. Atmos. Sci., 34, 911-921.
- Merrill, J.F., and J.E. Grant, 1979: A gravity wave-critical level encounter observed in the atmosphere. J. Geophys. Res., 84, 6315-6320.
- Morcrette, J.J., 1977: Calcul des flux infrarouges et des taux de refroidissement radiatif en atmosphere nuageuse. Thèse de spécialité, université des Sciences et techniques de Lille, n° 662, 123pp.
- Nicholls, S., and M.A. LeMone, 1980: The fair weather boundary layer in GATE: The relationship of subcloud fluxes and structure to the distribution and enhancement of cumulus clouds. J. Atmos. Sci., 37, 2051-2067.
- Nicholls, S., M.A. LeMone, and G. Sommeria, 1981: The simulation of a fair-weather marine boundary layer in GATE using a three-dimensional model. to appear in Quart. J. Roy. Meteor. Soc.
- Nitta, T., and S. Esbensen, 1974: Heat and moisture budgets analysis using BOMEX data. Mon. Wea. Rev., 102, 17-28.
- Nitta, T., 1976: Large-scale heat and moisture budgets during the air-mass transformation experiment. J. Met. Soc. Jap., 54, 1-14.
- O'Fiver, D.A., W.S. Lewellen, and G.G. Williamson, 1978: The interaction between turbulent and radiative transport in the development of fog and low-level stratus. J. Atmos. Sci., 35, 301-316.
- Pennel, W.T., and M.A. LeMone, 1974: An experimental study of turbulence structure in the fair weather trade-wind boundary layer. J. Atmos. Sci., 31, 1302-1323.
- Randall, D.A., 1980: Conditional instability of the first kind upside-down. J. Atmos. Sci., 37, 125-130.
- Randall, D.A., 1980: Entrainment in a stratocumulus layer with distributed radiative cooling. J. Atmos. Sci., 37, 148-159.
- Redelsperger, J.L., and G. Sommeria, 1981: Methode de représentation de la turbulence d'échelle inférieure à la maille pour un modèle 3-dimensionnel de convection nuageuse. To appear in Bound.-layer Meteor.
- Rothermel, J., and E.A. Agee, 1980: Aircraft investigation of mesoscale cellular convection during AMTEX 75. J. Atmos. Sci., 37, 1027-1040.
- Schertzer, D., and C. Simonin, 1981: A theoretical study of radiative cooling in homogeneous and isotropic turbulence. 3rd symposium Turbulent Shear Flows, Davies, Calif..
- Schubert, W.H., J.S. Wakefield, E.J. Steiner, and S.K. Cox, 1979: Marine stratocumulus convection. Part I: Governing equations and horizontally homogeneous solutions. J. Atmos. Sci., 36, 1286-1306.
- Simonin, O., 1981: Influence du transfert radiatif sur la turbulence de température. Thèse de Doctorat d'ingénieur, ENSTA, Paris.

- Sommeria, G., 1976: Three dimensional simulation of turbulent processes in an undisturbed trade wind boundary layer. J. Atmos. Sci., 33, 216-241.
- Sommeria, G., and J.W. Deardorff, 1977: Subgrid scale condensation in models of non-precipitating clouds. J. Atmos. Sci., 34, 345-355.
- Sommeria, G., and M.A. LeMone, 1978: Direct testing of a three dimensional model of the planetary boundary layer against experimental data. J. Atmos. Sci., 35, 25-39.
- Stephens, G.L., 1978: Radiation profiles in extended water clouds. II: Parameterization schemes. J. Atmos. Sci., 35, 2123-2132.
- Veyre, Ph., G. Sommeria, and Y. Fouquart, 1980: Modélisation de l'effet des hétérogénéités du champ radiatif infra-rouge sur la dynamique des nuages. J. Rech. Atmos., 14, 89-108.
- Wyngaard, J.C., and O.R. Coté, 1974: The evolution of a convective planetary boundary layer: A higher-order closure model study. Bound.-Layer Meteor., 7, 289-308.
- Yamada, T., and G.L. Mellor, 1979: A numerical simulation of BOMEX data using a turbulence closure model coupled with ensemble cloud relations. Quart. J. Roy. Meteor. Soc., 105, 915-944.
- Yanai, M., S. Esbensen, and J. Chu, 1973: Determination of bulk properties of tropical cloud clusters from large-scale heat and moisture budgets. J. Atmos. Sci., 30, 611-627.
- Zeman, O., and J.L. Lumley, 1976: Modeling buoyancy driven mixed-layers. J. Atmos. Sci., 33, 1974-1988.